CHEMISTRY OF MATERIALS
Article

Chem. Mater. **2010,** *22,* 6085–6091 6085
DOI:10.1021/cm101683c

High-Contrast Electrochromic Thin Films via Layer-by-Layer Assembly of Starlike and Sulfonated Polyaniline

Pengtao Jia,[†,‡] Avni A. Argun,[§] Jianwei Xu,[⊥] Shanxin Xiong,[‡] Jan Ma,[†,‡] Paula T. Hammond,*[,§] and Xuehong Lu*[,†,‡]

[†]*School of Materials Science and Engineering, Nanyang Technological University, 50 Nanyang Avenue, Singapore 639798,* [‡]*Temasek Laboratories, Nanyang Technological University, 50 Nanyang Drive, Singapore 637553,* [§]*Department of Chemical Engineering, Massachusetts Institute of Technology, Cambridge, Massachusetts 02139, United States, and* [⊥]*Institute of Materials Research and Engineering, 3 Research Link, Singapore 117602*

Received June 16, 2010. Revised Manuscript Received September 20, 2010

In this Article, we report the layer-by-layer (LbL) assembly and electrochromic properties of polyaniline-tethered cubic polyhedral oligomeric silsesquioxane (POSS-PANI)/sulfonated polyaniline (SPANI) multilayer thin films. The interaction between POSS-PANI and SPANI is characterized using X-ray photoelectron spectroscopy (XPS), ultraviolet−visible-near-infrared spectroscopy, and four-point probe conductivity. We show that the inclusion of SPANI during LbL assembly effectively dopes the underlying POSS-PANI layer and extends the conjugation length, as evidenced by probing the surface layers with XPS. We also demonstrate that the POSS-PANI/SPANI multilayer films have more electroactive units, lower band gap energies, and higher electrical conductivity values compared to those of POSS-PANI/poly(2-acrylamido-methane-2-propanesulfonic acid) (PAMPS) and spin-coated SPANI films. Under constant applied potentials, a 50 bilayer film of POSS-PANI/SPANI, $(POSS\text{-}PANI/SPANI)_{50}$, shows significant enhancement in optical contrast compared with $(POSS\text{-}PANI/PAMPS)_{50}$. Furthermore, the switching kinetics of $(POSS\text{-}PANI/SPANI)_{50}$ are much faster than that of the spin-coated SPANI. The improvement in electrochromic contrast under dynamic switching conditions is attributed to the presence of a larger number of electrochromic units in POSS-PANI/SPANI, the loose packing structure of POSS-PANI brought by its starlike molecular architecture, and the unique morphology created by the LbL assembly.

Introduction

Electrochromism is a phenomenon related to the reversible change in optical absorbance of a material induced by externally applied potential. In recent years, conjugated polymers have been increasingly studied as electrochromic materials due to their relatively high optical contrast, fast response speed, and wide range of colors.[1−6] Polymeric electrochromic thin films are commonly fabricated via spin-coating, solution-casting, or electropolymerization. An alternative approach is to fabricate electrochromic multilayer films using a layer-by-layer (LbL) assembly technique that allows facile incorporation of various functional materials into a thin film at a full range of compositions.[7] Many polymeric electrochromic multilayer films, such as polyaniline (PANI)/poly(2-acrylamido-methane-2-propanesulfonic acid) (PAMPS),[8] PANI/poly(sodium styrenesulfonate),[9] PANI/poly(vinyl sulfonate),[9] triarylamine polymers/poly(choline methacrylate),[10] poly(ethylene imine)/poly(3,4-ethylenedioxythiophene),[11] and poly(4-(2,3-dihydrothieno[3,4-*b*][1,4]-dioxin-2-yl-methoxy)-1-butanesulfonic acid/poly(allylamine hyrochloride),[12] have been reported. We have recently reported the synergistic combination of the starlike structure of polyaniline tethered polyhedral oligomeric silsesquioxane nanocage (POSS-PANI), finding that the LbL assembly greatly facilitates the electrochromic switching and improves the contrast of the electrochromic multilayer films under dynamic switching conditions.[13] In addition, the switching kinetics of the multilayer POSS-PANI films is much faster than that of spin-coated thin films. In all the studies described above, the electrochromic multilayer films are, however,

*Corresponding author. Tel.: +65 6790 4585 (X.L.). Fax: +65 6790 9081 (X.L.). E-mail: asxhlu@ntu.edu.sg (X.L.); hammond@mit.edu (P.T.H.).

(1) Beaujuge, P. M.; Reynolds, J. R. *Chem. Rev.* **2010**, *110*, 268.
(2) Wang, X. B.; Ng, J. K. P.; Jia, P. T.; Lin, T. T.; Cho, C. M.; Xu, J. W.; Lu, X. H.; He, C. B. *Macromolecules* **2009**, *42*, 5534.
(3) Wu, C. G.; Lu, M. I.; Chang, S. J.; Wei, C. S. *Adv. Funct. Mater.* **2007**, *17*, 1063.
(4) Sapp, S. A.; Sotzing, G. A.; Reynolds, J. R. *Chem. Mater.* **1998**, *10*, 2101.
(5) Sonmez, G.; Meng, H.; Zhang, Q.; Wudl, F. *Adv. Funct. Mater.* **2003**, *13*, 726.
(6) Mortimer, R. J.; Dyer, A. L.; Reynolds, J. R. *Displays* **2006**, *27*, 2.
(7) Decher, G. *Science* **1997**, *277*, 1232.
(8) DeLongchamp, D.; Hammond, P. T. *Adv. Mater.* **2001**, *13*, 1455.
(9) Chen, Y. H.; Wu, J. Y.; Chung, Y. C. *Biosens. Bioelectron.* **2006**, *22*, 489.
(10) Choi, K.; Yoo, S. J.; Sung, Y. E.; Zentel, R. *Chem. Mater.* **2006**, *18*, 5823.
(11) Tang, Z. X.; Donohoe, S. T.; Robinson, J. A.; Chiarelli, P. A.; Wang, H. L. *Polymer* **2005**, *46*, 9043.
(12) Cutler, C. A.; Bouguettaya, M.; Kang, T. S.; Reynolds, J. R. *Macromolecules* **2005**, *38*, 3068.
(13) Jia, P. T.; Argun, A. A.; Xu, J. W.; Xiong, S. X.; Ma, J.; Hammond, P. T.; Lu, X. H. *Chem. Mater.* **2009**, *21*, 4434.

Published on Web 10/20/2010

composed of alternating layers of conjugated-polymer and polymeric dopant/electrolyte; the latter is electrically inactive and, hence, cannot contribute to the electrochromic contrast. To further enhance the electrochromic contrast of the multilayer thin films, a plausible approach is to fabricate fully conjugated polymeric multilayer films, in which both polycation and polyanion layers exhibit electrochromic activity. So far, only a cathodically colored polymer pair, poly(hexyl viologen)/poly(3,4-ethylenedioxythiophene)−poly(styrene sulfonate),[14] has been assembled to include multiple chromophores. A good candidate for an anodically colored polymer pair is PANI/highly sulfonated PANI (self-doped PANI, SPANI) since both polymers show promising electrochromic characteristics and can play an active role. PANI is the most widely used anodically coloring electrochromic polymer due to its ease of synthesis and good environmental stability,[15,16] and the absorption band of SPANI overlaps well with the emeraldine salt form of PANI.[17,18]

A few groups have previously reported LbL-assembled PANI/SPANI multilayer films for sensor applications.[19−21] Despite their stability,[19] the redox process within the PANI/SPANI multilayer film is slowed by diffusion limitations and a high degree of ionic cross-linking,[19] far from ideal conditions for dynamically switching electrochromic devices. Furthermore, the motivation to use highly sulfonated SPANI is to increase the content of active units in the multilayer film, which is based on the assumption that some sulfonic acid groups on SPANI chains are able to dope PANI chains to increase the reversible redox capability of PANI without disturbing the conjugated structure of SPANI. To date, no direct experimental evidence for such interchain doping has been reported and it is not clear how such interchain interactions will affect electrochromic properties of multilayer films. In the present work, to improve the switching kinetics, we show the fabrication of multilayer films based on a starlike POSS-PANI polycation, which can induce a loose interchain packing structure,[22] paired with highly sulfonated SPANI. We correlate the structure and morphology of POSS-PANI/SPANI films to their electrochemical properties and electrochromic behaviors under both constant potential and dynamic switching conditions. In addition, we use X-ray photoelectron spectroscopy (XPS) and ultraviolet−visible-near-infrared (UV−vis-NIR) spectroscopy to probe the doping states of the aniline unit in SPANI and POSS-PANI/SPANI multilayer films, as well as the interaction between the two components in the multilayer films.

Experimental Section

Chemicals. Aniline, SPANI (degree of sulfonation of ∼100%, $M_n = 10\,000$), PAMPS (M_w of ∼2 000 000), acetonitrile (99.5%), *N*,*N*-dimethylacetamide (≥99%), lithium perchlorate (≥95.0%), and ferrocene (98%) were purchased from Aldrich. Aniline was purified by vacuum distillation prior to use. Octa(aminophenyl) silsesquioxane (OAPS) was purchased from Mayaterials Inc. and purified to reduce the content of octa(nitrophenyl) silsesquioxane prior to use. The emeraldine base form of POSS-PANI was prepared from OAPS (1 mol.%) and aniline (99 mol.%) according to our previous publication.[13] Other chemicals were obtained from various commercial sources and used as received.

Preparation of Dipping Solutions. POSS-PANI and PAMPS solutions were prepared according to our previous publication.[13] SPANI solution (0.78 mM) was prepared by dissolving SPANI in water under stirring, and the pH value of the SPANI aqueous solution was adjusted to 2.5.

LbL Assembly of Multilayer Thin Films. Multilayer thin films were constructed using a HMS 70 slide stainer. The substrate treatment procedure was the same as the previously reported procedure.[13] Indium tin oxide (ITO)-glass, uncoated glass, and silicon substrates were exposed first to POSS-PANI solution for 15 min, followed by three consecutive rinsing steps (1.5 min, 1.5 min, 1.5 min) in Milli-Q water, and then exposed to SPANI solution for 5 min or PAMPS solution for 15 min and rinsed. The cycle was repeated to create multilayer thin films of certain thickness. The pH value of all the rinsing solutions was adjusted to 2.50. Fifteen bilayers of POSS-PANI/SPANI ((POSS-PANI/SPANI)$_{15}$) with SPANI on top and 15.5 bilayers of POSS-PANI/SPANI ((POSS-PANI/SPANI)$_{15.5}$) with POSS-PANI on top were assembled, and a SPANI thin film of 30 nm thickness was spin-coated on silicon wafer for XPS measurements. For other tests, multilayer films of 50 bilayers of POSS-PANI/SPANI ((POSS-PANI/SPANI)$_{50}$) were assembled. POSS-PANI/PAMPS multilayer films of 50 bilayers (POSS-PANI/PAMPS)$_{50}$) and a spin-coated SPANI film of 100 nm thickness were also fabricated as reference samples.

Thin Film Characterization. Thickness measurements were performed with an Alfa-step Q surface profiler. XPS experiments were performed using a VG ESCALAB 220i-XL instrument equipped with a monochromatic Al Kα X-ray source (1486.7 eV photons). To compensate for surface-charging effects, all binding energies were referenced to the C(1s) neutral carbon peak at 285.0 eV. In curve fitting, all core-level spectra were deconvoluted into Gaussian component peaks and the line width (full-width at half-maximum, fwhm) of the Gaussian peaks was maintained constant for all components and the Shirley background was subtracted. The stoichiometries of S/N were determined from their peak area ratio after correcting with the sensitivity factors. A four-point probe system (Signatone SP4-62.5-85-TC) was used to measure the surface electrical conductivity of the polymer films. Wide angle X-ray diffraction (WAXD) measurements were performed using a Shimadzu 6000 X-ray diffractometer with Cu Kα radiation. All of the samples were scanned from 10° to 45° 2θ. Atomic force microscope (AFM) measurements were performed in tapping mode using a Digital Instruments Nanoscope 3100 AFM. Electrochemical properties and in situ spectro-electrochemical properties of the multilayer thin films were characterized using an Autolab PGSTAT30 electrochemical workstation and Perkin-Elmer UV−vis-NIR

(14) DeLongchamp, D. M.; Kastantin, M.; Hammond, P. T. *Chem. Mater.* **2003**, *15*, 1575.
(15) Jia, P.; Xu, J.; Ma, J.; Lu, X. *Eur. Polym. J.* **2009**, *45*, 772.
(16) Xiong, S. X.; Phua, S. L.; Dunn, B. S.; Ma, J.; Lu, X. H. *Chem. Mater.* **2010**, *22*, 255.
(17) Yang, C. H.; Chih, Y. K.; Wu, W. C.; Chen, C. H. *Electrochem. Solid-State Lett.* **2006**, *9*, C5.
(18) Li, C.; Mu, S. *Synth. Met.* **2004**, *144*, 143.
(19) Tian, S. J.; Baba, A.; Liu, J. Y.; Wang, Z. H.; Knoll, W.; Park, M. K.; Advincula, R. *Adv. Funct. Mater.* **2003**, *13*, 473.
(20) Zhang, N.; Schweiss, R.; Knoll, W. *J. Solid State Electrochem.* **2007**, *11*, 451.
(21) Baba, A.; Park, M. K.; Advincula, R. C.; Knoll, W. *Langmuir* **2002**, *18*, 4648.
(22) Xiong, S.; Xiao, Y.; Ma, J.; Zhang, L.; Lu, X. *Macromol. Rapid Commun.* **2007**, *28*, 281.

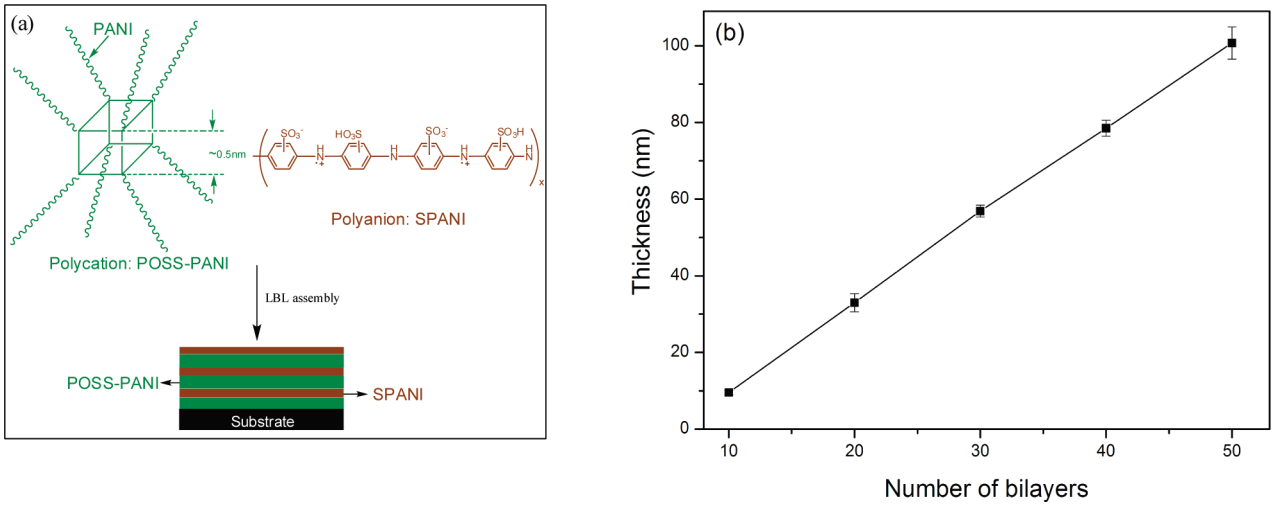

Figure 1. (a) Scheme showing the structure of POSS-PANI/SPANI multilayer films and (b) the growth curve for LbL assembly of POSS-PANI/SPANI multilayer films on glass.

spectrophotometer. The electrochromic thin films on ITO-glass were positioned in a quartz cell with electrolyte as working electrodes. The electrolyte is 0.1 M $LiClO_4$ in acetonitrile. Platinum wire (99.99%) and silver wire (99.9%) were used as counter and reference electrode, respectively. The pseudoreference silver wire was calibrated vs. Fc/Fc^+ by dissolving ferrocene in the electrolyte solution and determining the $E_{1/2}$ of the Fc/Fc^+ against the silver wire.

Results and Discussion

LbL Assembly of the Multilayer Thin Films. The LbL assembly process can create macromolecular complexes by alternating exposure of a substrate to dilute aqueous solutions or dispersions of materials with attractive affinities.[14,23,24] The LbL assembly scheme for this work is shown in Figure 1a. In order to make a fair comparison between POSS-PANI/SPANI and POSS-PANI/PAMPS, the dipping time and concentration of SPANI polyanion solution are controlled to ensure that the thickness of each bilayer is about 2.0 nm, similar to that of POSS-PANI/PAMPS.[13] Figure 1b shows that the LbL growth of POSS-PANI/SPANI multilayer films as a function of bilayer number is linear under the conditions used. The thickness of $(POSS\text{-}PANI/SPANI)_{50}$, $(POSS\text{-}PANI/PAMPS)_{50}$, and spin-coated SPANI are all controlled to be 100 nm.

For the system under study, electrostatic interaction between the sulfonic acid groups attached to the backbone of SPANI and the cationic amine nitrogen groups in POSS-PANI provide the driving force for the LbL assembly. To study the interaction between POSS-PANI and SPANI, XPS is used to probe the different states of nitrogen and to determine the proportion of these species to the total amount of nitrogen atoms.[25−30] In order to differentiate the different states of cationic nitrogen, a N 1s peak was analyzed using the peak fitting method. The XPS spectra and the fitting curves for N 1s peaks are given in the Supporting Information (cf. Figure S1). The data obtained from the curve fitting are summarized in Table 1.

In the XPS spectra, the peaks at about 400 eV are due to the undoped amine units. The peaks at about 401 eV are associated with cationic nitrogen atoms at polaron and bipolaron states, while the peaks at about 402 eV are correlated to sp^3 protonated amine units. The latter occurs at a higher binding energy because of the stronger electron localization associated with poorer conjugation.[25,31] When one layer of POSS-PANI is deposited onto the multilayer film of 15 bilayers ($(POSS\text{-}PANI/SPANI)_{15}$), the proportion of polaron and bipolaron cationic nitrogen increases from 28.3% for $(POSS\text{-}PANI/SPANI)_{15}$ to 30.5% for $(POSS\text{-}PANI/SPANI)_{15.5}$, while the proportion of high-binding-energy protonated amine decreases from 12.8% for $(POSS\text{-}PANI/SPANI)_{15}$ to 9.9% for $(POSS\text{-}PANI/SPANI)_{15.5}$. The chemical composition of the probed surface for $(POSS\text{-}PANI/SPANI)_{15}$ and $(POSS\text{-}PANI/SPANI)_{15.5}$ is unchanged according to the XPS analysis from the corrected N 1s and S 2p core-level spectral area ratio (cf. Supporting Information, Figure S2), indicating that the observed difference is due to the change in ionic bonding. We attribute this difference to the reorganization of SPANI chains to effectively dope POSS-PANI to form more polarons and bipolarons, which is accompanied by a decrease in the amount of protonated amine units in SPANI layers. Since the protonated amine units interfere with the formation of polarons and bipolarons to interrupt the order of the polaron lattice,[32,33] the decrease in the amount of protonated amine units extends

(23) DeLongchamp, D. M.; Hammond, P. T. *Chem. Mater.* **2004**, *16*, 4799.
(24) Advincula, R. C.; Fells, E.; Park, M. K. *Chem. Mater.* **2001**, *13*, 2870.
(25) Wei, X. L.; Fahlman, M.; Epstein, K. J. *Macromolecules* **1999**, *32*, 3114.
(26) Han, M. G.; Im, S. S. *Polymer* **2000**, *41*, 3253.
(27) Jousseaume, V.; Morsli, M.; Bonnet, A.; Lefrant, S. *J. Appl. Polym. Sci.* **1998**, *67*, 1209.
(28) Nicolau, Y. F.; Ermolieff, A. *Synth. Met.* **1995**, *71*, 2073.
(29) Kang, E. T.; Neoh, K. G.; Tan, K. L. *Synth. Met.* **1995**, *68*, 141.
(30) Chen, S. A.; Hwang, G. W. *J. Am. Chem. Soc.* **1995**, *117*, 10055.
(31) Yue, J.; Epstein, A. J.; Macdiarmid, A. G. *Mol. Cryst. Liq. Cryst.* **1990**, *189*, 255.
(32) Jiang, Y.; Epstein, A. J. *J. Am. Chem. Soc.* **1990**, *112*, 2800.
(33) Kang, E. T.; Neoh, K. G.; Woo, Y. L.; Tan, K. L. *Polymer* **1992**, *33*, 2857.

Table 1. N 1s Data of Various Samples Obtained from XPS Analysis

Peak and proportion		Spin-coated SPANI	(POSS-PANI/SPANI)$_{15}$	(POSS-PANI/SPANI)$_{15.5}$
N1s binding energy (eV)		399.6	399.9	399.8
	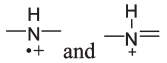	401.1	400.9	400.9
		402.1	402.2	402.2
N1s proportion (%)[a]		40.6	58.9	59.6
	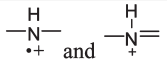	19.4[b]	28.3	30.5
		40.0	12.8	9.9

[a] The values were determined via the curve-fitting of N 1s core-level spectra of spin-coated SPANI of 30 nm thickness, (POSS-PANI/SPANI)$_{15}$ and (POSS-PANI/SPANI)$_{15.5}$. [b] For spin-coated SPANI, the value is determined from the cationic nitrogen atoms at polaron state.

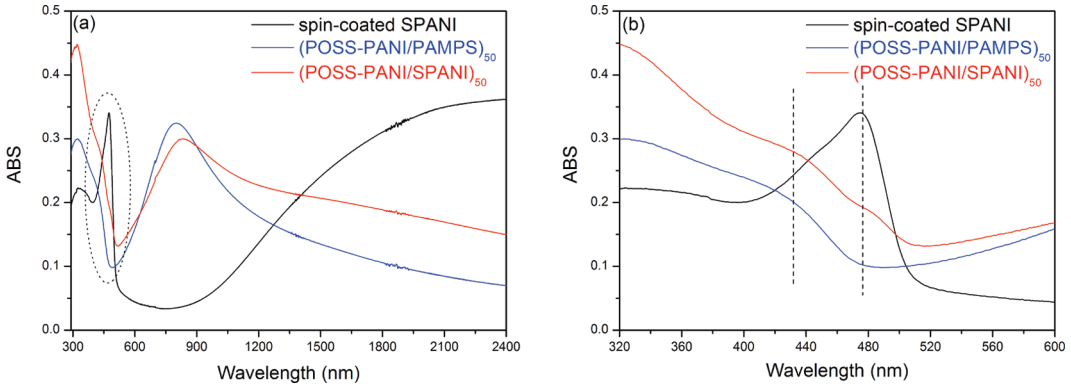

Figure 2. (a) UV−vis-NIR spectra of the spin-coated SPANI (black), (POSS-PANI/PAMPS)$_{50}$ (blue), and (POSS-PANI/SPANI)$_{50}$ (red). (b) Polaron absorption peaks of the spin-coated SPANI, (POSS-PANI/PAMPS)$_{50}$, and (POSS-PANI/SPANI)$_{50}$.

the conjugated π system in POSS-PANI/SPANI thin film and facilitates redox switching.

The extension of conjugation also influences band gap energies and electrical conductivity values of the polymer films. UV−vis-NIR spectra of the spin-coated SPANI, (POSS-PANI/PAMPS)$_{50}$, and (POSS-PANI/SPANI)$_{50}$ are shown in Figure 2a. The peaks at about 800 nm for (POSS-PANI/PAMPS)$_{50}$ and (POSS-PANI/SPANI)$_{50}$ are due to the trapped excitons centered on quinoid moieties,[34] which do not appear in the spectrum of the spin-coated SPANI. The peak at about 430 nm for (POSS-PANI/PAMPS)$_{50}$ and at 475 nm for the spin-coated SPANI are due to polaron absorption.[30,34] When the polaron absorption peaks are enlarged (Figure 2b), two weak polaron peaks can be observed from the spectrum of (POSS-PANI/SPANI)$_{50}$. When these two peaks are compared with the polaron peaks of the spin-coated SPANI and (POSS-PANI/PAMPS)$_{50}$, one polaron peak for (POSS-PANI/SPANI)$_{50}$ can be assigned to POSS-PANI while the other is assigned to the SPANI component. In order to calculate band gap energies, plots of $(\alpha h\nu)^2$ versus $h\nu$[16,35−38] are obtained for the spin-coated SPANI, (POSS-PANI/PAMPS)$_{50}$ and (POSS-PANI/SPANI)$_{50}$ (cf. Supporting Information, Figure S3). As shown in Table 2, the band gap of POSS-PANI decreases from 2.60 eV

Table 2. Band Gap and Electrical Conductivity

Materials	Band gap (eV)	Electrical conductivity (S/cm)
Spin-coated SPANI	2.47	4.65×10^{-3}
(POSS-PANI/SPANI)$_{50}$	2.36, 2.48	1.15×10^{-2}
(POSS-PANI/PAMPS)$_{50}$	2.60	2.55×10^{-3}

(34) Tzou, K.; Gregory, R. V. *Synth. Met.* **1993**, *53*, 365.
(35) lekha, P. C.; Subramanian, E.; Padiyan, D. P. *Sens. Actuators, B* **2007**, *122*, 274.
(36) De, S.; Dey, A.; De, S. K. *J. Phys. Chem. Solids* **2007**, *68*, 66.
(37) Yakuphanoglu, F.; Senkal, B. F.; Sarac, A. *J. Electron. Mater.* **2008**, *37*, 930.
(38) Subramanian, S.; Chithra lekha, P.; Pathinettam Padiyan, D. *Curr. Appl. Phys.* **2009**, *9*, 1140.

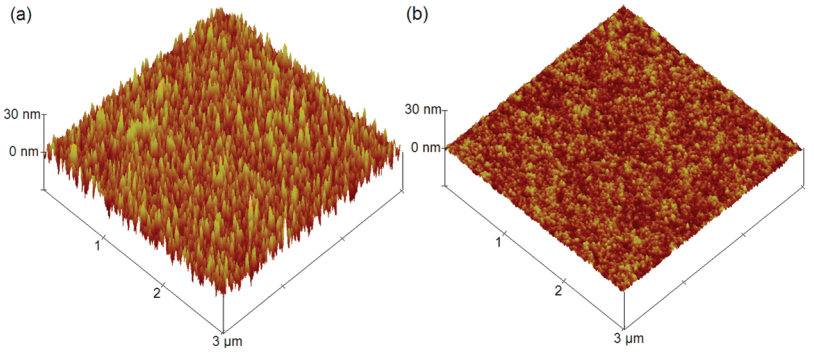

Figure 3. Tapping-mode AFM images of (a) $(POSS\text{-}PANI/SPANI)_{15}$ with SPANI on top and (b) the spin-coated SPANI thin film with 30 nm thickness.

in $(POSS\text{-}PANI/PAMPS)_{50}$ to 2.48 eV in $(POSS\text{-}PANI/SPANI)_{50}$ and the band gap of SPANI decreases from 2.47 eV in the spin-coated SPANI to 2.36 eV in $(POSS\text{-}PANI/SPANI)_{50}$. In addition, the electrical conductivity of $(POSS\text{-}PANI/SPANI)_{50}$ is an order of magnitude higher than those of spin-coated SPANI and $(POSS\text{-}PANI/PAMPS)_{50}$ films (Table 2). WAXD results (cf. Supporting Information, Figure S4) show that all three thin films are dominantly amorphous and their differences in electrical conductivity values are not due to their difference in degree of crystallinity or crystal size. The lower band gap and higher electrical conductivity of $(POSS\text{-}PANI/SPANI)_{50}$, thus, confirm the strong interaction between POSS-PANI and SPANI which extends the conjugation in POSS-PANI/SPANI films and may significantly influence electrochromic properties of $(POSS\text{-}PANI/SPANI)_{50}$.

Surface Morphology. The surface roughness of SPANI terminated $(POSS\text{-}PANI/SPANI)_{15}$ and POSS-PANI terminated $(POSS\text{-}PANI/SPANI)_{15.5}$ multilayer films, as well as that of a spin-coated SPANI film, was examined using AFM. The surface of the SPANI terminated multilayer film is significantly rougher than the spin-coated SPANI film as shown in Figure 3. $(POSS\text{-}PANI/SPANI)_{15.5}$ shows a similar rough morphology to that of $(POSS\text{-}PANI/SPANI)_{15}$ (cf. Supporting Information, Figure S5). This observation supports the concept that the starlike structure of POSS-PANI yields a rougher, mesoporous morphology and, hence, provides a larger interaction between the PANI and SPANI layers.

Cyclic Voltammetry (CV). CV studies show that the oxidation and reduction peaks in CV curves of $(POSS\text{-}PANI/SPANI)_{50}$ are more distinct than those of the spin-coated SPANI (cf. Supporting Information, Figure S6), which implies that the redox process in the $(POSS\text{-}PANI/SPANI)_{50}$ multilayer thin film is faster than the spin-coated SPANI. Comparing the CV curves of the spin-coated SPANI and $(POSS\text{-}PANI/SPANI)_{50}$, as well as that of $(POSS\text{-}PANI/PAMPS)_{50}$ (Figure 4), the transition between the emeraldine and pernigraniline state is shifted to lower potentials for $(POSS\text{-}PANI/SPANI)_{50}$ compared with those of $(POSS\text{-}PANI/PAMPS)_{50}$, indicating a more favorable electrochemical reaction. Furthermore, $(POSS\text{-}PANI/SPANI)_{50}$ shows only one transition in this region (instead of two peaks corresponding to transitions from POSS-PANI and SPANI), which demonstrates that the

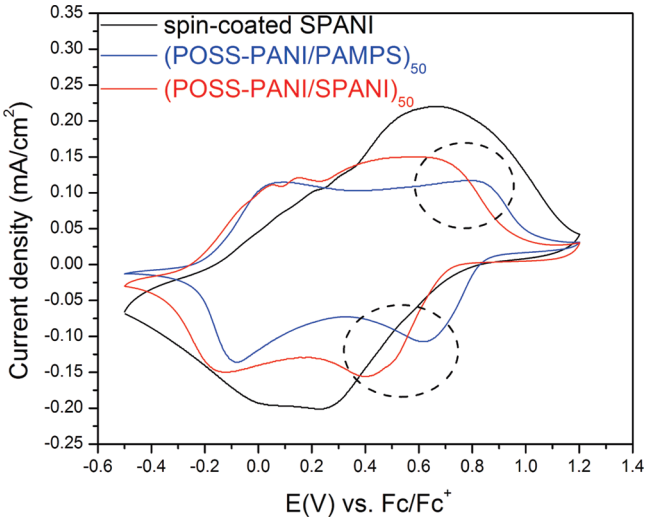

Figure 4. CV curves of spin-coated SPANI (black), $(POSS\text{-}PANI/PAMPS)_{50}$ (blue), and $(POSS\text{-}PANI/SPANI)_{50}$ (red) measured in a 0.1 M $LiClO_4$/acetonitrile solution at the scan rate of 25 mV/s.

interaction between POSS-PANI and SPANI has altered the electrochemical properties of both components. The strong interaction between POSS-PANI and SPANI layers results in shifting of oxidation and reduction potentials to lower values, making this system more accessible. This is further proven by analyzing the scan rate dependence of current, which shows that the redox processes in $(POSS\text{-}PANI/SPANI)_{50}$ films are not diffusion-controlled, in contrast to the spin-coated SPANI film[39,40] (cf. Supporting Information, Figure S6).

Spectro-Electrochemical Characterization. Spectroelectrochemistry plays a key role in examining the optical changes that occur upon doping or dedoping of an electrochromic film. Figure 5 shows two series of UV−vis absorbance spectra of $(POSS\text{-}PANI/SPANI)_{50}$ and the spin-coated SPANI under various applied potentials varying from −0.4 V to +0.8 V vs Fc/Fc^+. $(POSS\text{-}PANI/SPANI)_{50}$ can be switched between a relatively transmissive reduced state (yellowish green) and an absorbing oxidized state (blue) (cf. Supporting Information, Figure S7). The maximum change in absorbance (ΔA) of $(POSS\text{-}PANI/SPANI)_{50}$ ($\Delta A = 0.25$ at 592 nm;

(39) Kogan, I. L.; Gedrovich, G. V.; Fokeeva, L. S.; Shunina, I. G. *Electrochim. Acta* **1996**, *41*, 1833.
(40) Xiong, S. X.; Jia, P. T.; Mya, K. Y.; Ma, J.; Boey, F.; Lu, X. H. *Electrochim. Acta* **2008**, *53*, 3523.

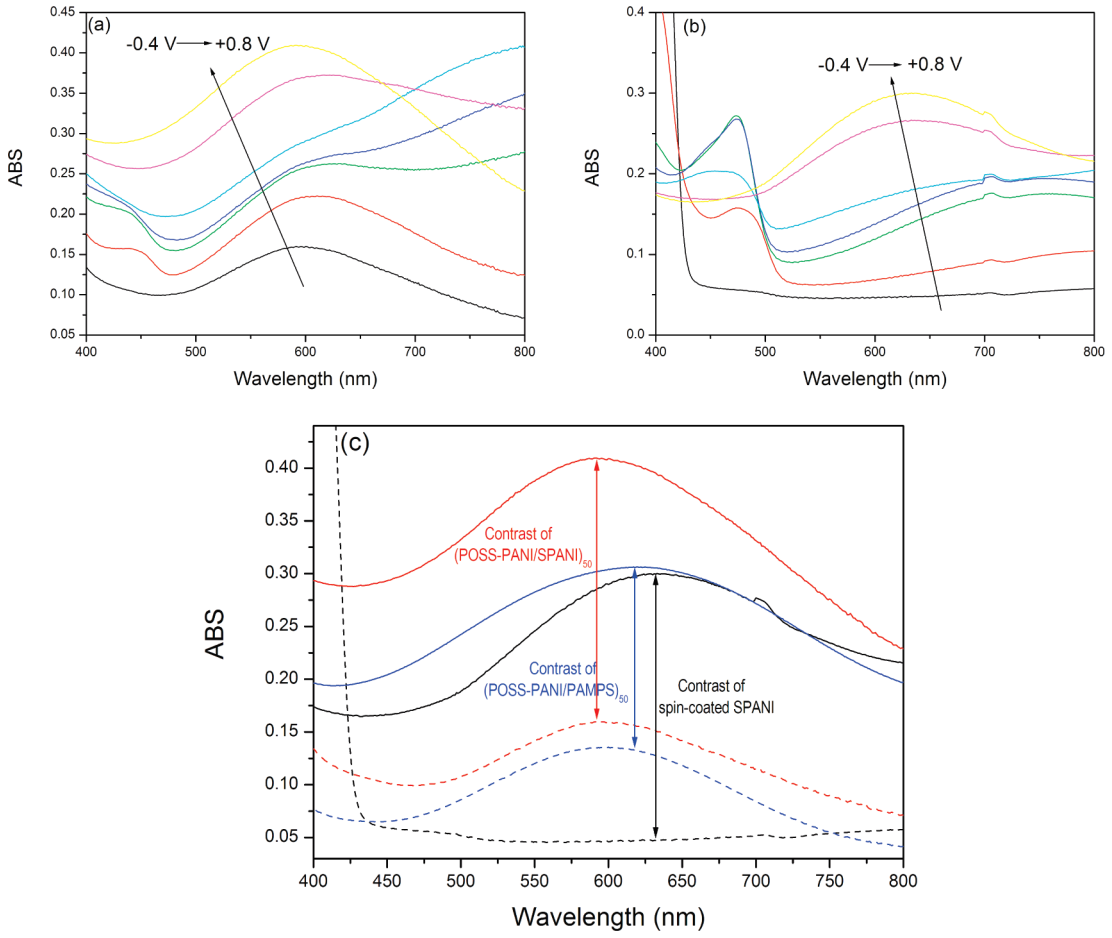

Figure 5. Visible spectra of (a) $(POSS\text{-}PANI/SPANI)_{50}$ and (b) the spin-coated SPANI under different potentials (−0.4, −0.1, +0.1, +0.2, +0.4, +0.6, and +0.8 V). (c) The visible spectra of $(POSS\text{-}PANI/SPANI)_{50}$ (red), $(POSS\text{-}PANI/PAMPS)_{50}$ (blue), and the spin-coated SPANI (black) under +0.8 V (solid lines) and −0.4 V (dashed lines).

Figure 5a) is the same as that of the spin-coated SPANI (ΔA = 0.25 at 630 nm; Figure 5b). Comparing the absorbance curves under +0.8 and −0.4 V for $(POSS\text{-}PANI/SPANI)_{50}$ with those of $(POSS\text{-}PANI/PAMPS)_{50}$ (Figure 5c), the maximum contrast of $(POSS\text{-}PANI/SPANI)_{50}$ is much higher than that of $(POSS\text{-}PANI/PAMPS)_{50}$ as both components in $(POSS\text{-}PANI/SPANI)_{50}$ can contribute to the electrochromic contrast. The wavelength corresponding to the maximum absorbance for $(POSS\text{-}PANI/SPANI)_{50}$ is shifted to a slightly lower wavelength in comparison with that of $(POSS\text{-}PANI/PAMPS)_{50}$, suggesting that $(POSS\text{-}PANI/SPANI)_{50}$ multilayer film can be more easily oxidized.[16] This is consistent with the CV observation that the oxidation peak potential for the $(POSS\text{-}PANI/SPANI)_{50}$ multilayer film is lower than that of $(POSS\text{-}PANI/PAMPS)_{50}$.

Potential Step Absorptometry. The optical switching behaviors of the multilayer films are examined at wavelengths corresponding to their maximum change in absorbance (λ_{max}) using an UV−vis-NIR spectrophotometer with the applied potential stepped between −0.4 V and +0.8 V at 60 s per cycle. It is striking to see that the contrast of $(POSS\text{-}PANI/SPANI)_{50}$ (ΔA=0.26) is significantly higher than those of both $(POSS\text{-}PANI/PAMPS)_{50}$ (ΔA=0.19) and the spin-coated SPANI (ΔA=0.15) under such a dynamic switching condition (Figure 6). To understand why the

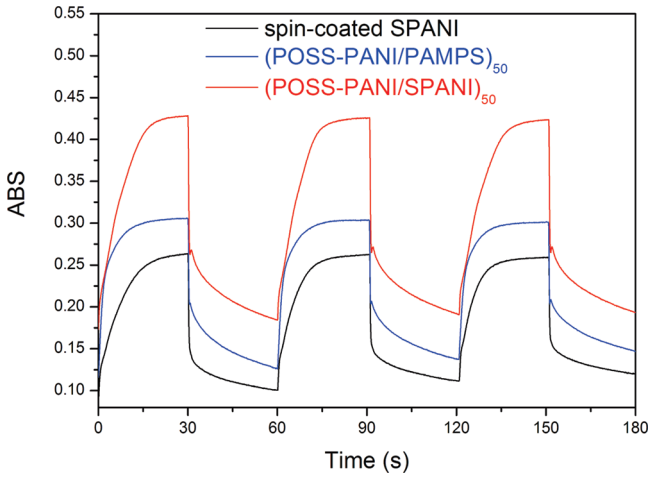

Figure 6. Potential step absorptometry of $(POSS\text{-}PANI/SPANI)_{50}$ (red), $(POSS\text{-}PANI/PAMPS)_{50}$ (blue), and the spin-coated SPANI (black). The thickness of all three films are 100 nm.

contrast of the spin-coated SPANI is approximately the same as that of $(POSS\text{-}PANI/SPANI)_{50}$ under constant applied potentials while it is much lower under the dynamic switching condition, it is necessary to compare Figure 5c with Figure 6. The comparison data are listed in Table 3. The absorbance maximum of the spin-coated SPANI measured under the dynamic condition (A = 0.26) is lower than that

Table 3. Wavelength Corresponding to the Maximum Absorbance (ABS λ_{max}) and Optical Contrast of All Samples

materials	ABS λ_{max} (nm)	contrast measured using the chronoamperometric method	contrast measured under the step potential
spin-coated SPANI	630	0.25 (from 0.30 to 0.05)	0.15 (from 0.26 to 0.11)
$(POSS\text{-}PANI/SPANI)_{50}$	592	0.25 (from 0.41 to 0.16)	0.26 (from 0.43 to 0.17)
$(POSS\text{-}PANI/PAMPS)_{50}$	626	0.17 (from 0.30 to 0.13)	0.19 (from 0.31 to 0.12)

measured using the chrono amperometric method (A=0.30), and the absorbance minimum of SPANI measured under the dynamic condition (A = 0.11) is higher than that measured using the chrono amperometric method (A=0.05), indicating that a significant part of SPANI units is not accessible under the dynamic switching condition, and therefore cannot be switched. Since the redox process in the spin-coated SPANI is diffusion controlled, there is enough time during chrono amperometric measurements for the doping ions to diffuse in and out of the SPANI film so that the redox process can be fully completed. However, under a dynamic switching condition of 60 s, there is not enough time for the doping ions to move in and out of spin-coated SPANI film. Thus, during the dynamic switching, the redox process in the spin-coated SPANI film cannot finish completely in 60 s, which leads to the lower contrast of the spin-coated SPANI under the dynamic switching condition. The contrast values of $(POSS\text{-}PANI/SPANI)_{50}$ and $(POSS\text{-}PANI/PAMPS)_{50}$ are almost unchanged whether the measurement method is chrono amperometric or dynamic switching, indicating that all PANI units are easily accessible and can be switched within 60 s. Thus, the significantly higher contrast achieved with POSS-PANI/SPANI can be attributed to the greater amount of active units induced by interchain interaction between POSS-PANI and SPANI, the loosely packed structure of POSS-PANI brought by its starlike molecular architecture, and the unique morphology created by the LbL assembly that facilitates the ion transport during the redox reactions.

Conclusions

In summary, POSS-PANI/SPANI multilayer thin films have been successfully fabricated via the LbL assembly technique. XPS analysis shows that there is strong interaction between POSS-PANI and SPANI that increases the amount of electroactive units and extends the conjugation length in POSS-PANI/SPANI. This interaction leads to lower band gap energies and higher electrical conductivity values compared with the values obtained from underlying components POSS-PANI and neat spin-cast films of SPANI. On the basis of the CV studies, the interaction between POSS-PANI and SPANI has also altered the electrochemical properties of POSS-PANI and SPANI components. The oxidation and reduction potentials have been shifted to lower values, resulting in a more favorable redox reaction for the LbL assembled POSS-PANI/SPANI system. Furthermore, as opposed to the spin-coated SPANI film, the redox processes in the POSS-PANI/SPANI multilayer thin film are not diffusion-controlled. Finally, the electrochromic contrast of POSS-PANI/SPANI is increased by more than 35% over that of POSS-PANI/PAMPS, and the switching kinetics of the POSS-PANI/SPANI multilayer film is much faster than that of the spin-coated SPANI. These findings indicate that the LbL method can be used to actually enhance the functional properties of polymers via intimate blending with synergistic polyions. In the case demonstrated here, the combination of a starlike conjugated molecular architecture and the self-doping and ionically conductive aspects of SPANI, brought together through the use of LbL assembly, has proven effective in achieving high contrast and fast switching electrochromic polymer films. We believe that this approach is easily adaptable to other conjugated polymer systems and, thus, has significant potential for future applications of conjugated polymers in electrochromic and electrochemical devices.

Acknowledgment. P.J. thanks Nanyang Technological University, Singapore, for providing his Ph.D. scholarship in the course of this work.

Supporting Information Available: XPS N 1s of the spin-coated SPANI thin film with 30 nm thickness, $(POSS\text{-}PANI/SPANI)_{15}$ and $(POSS\text{-}PANI/SPANI)_{15.5}$; plots of the corrected N1s and S2p core-level spectra for $(POSS\text{-}PANI/SPANI)_{15}$ and $(POSS\text{-}PANI/SPANI)_{15.5}$; plot of $(\alpha h\nu)^2$ versus $h\nu$ for spin-coated SPANI with 100 nm thickness, $(POSS\text{-}PANI/PAMPS)_{50}$ and $(POSS\text{-}PANI/SPANI)_{50}$; X-ray diffraction patterns of spin-coated SPANI with 100 nm thickness, $(POSS\text{-}PANI/PAMPS)_{50}$ and $(POSS\text{-}PANI/SPANI)_{50}$; tapping-mode AFM image of $(POSS\text{-}PANI/SPANI)_{15.5}$ with POSS-PANI on top; CV curves of $(POSS\text{-}PANI/SPANI)_{50}$ and the spin-coated SPANI measured in a 0.1 M $LiClO_4$/acetonitrile solution; plots of peak current densities vs scan rate and plots of peak current densities vs square root of scan rate; photographs of $(POSS\text{-}PANI/SPANI)_{50}$ in (a) reduced state and (b) oxidized state measured in a 0.1 M $LiClO_4$/acetonitrile solution (PDF). This material is available free of charge via the Internet at http://pubs.acs.org.